Bulletin of Electrical Engineering and Informatics
Vol. 12, No. 5, October 2023, pp. 2913~2922
ISSN: 2302-9285, DOI: 10.11591/eei.v12i5.5011

Enhancement of DWT-SVD digital image watermarking against noise attack using time–frequency representation

Mohanad Najm Abdulwahed, Ali Kamil Ahmed
Department of Materials Engineering, University of Technology, Baghdad, Iraq

Article Info

Article history:

Received Oct 14, 2022
Revised Dec 16, 2022
Accepted Feb 16, 2023

Keywords:

Denoising
Encryption
Noise
Time-frequency
Wavelet

ABSTRACT

Information security has been defined as one of the most critical issues in the information era, as it is utilized to protect confidential information during transfers in real-world applications. In the case of image encryption, a variety of information security approaches were used. Domain spatial and domain frequency are two domains in which such techniques can be classified. This study uses a combination of the singular value de-composition (SVD) and discrete wavelet transformation (DWT) to construct an encryption method based on a traditional watermarking system. Compared with other traditional methods, the proposed DWT-SVD approach has excellent robustness, and it has been strengthened for having high degree of the robustness against the additive white Gaussian noise (AWGN) attacks by utilizing a de-noising strategy based upon S-transform approach. Compared with DWT algorithm denoising approach, the results reveal that the S-transform denoising algorithm that has been deployed in the present article has a robust protection towards the Gaussian noise attack for mean squared error (MSE) around 0.005 and peak signal to noise ratio (PSNR) around 24 dB.

Corresponding Author:

Mohanad Najm Abdulwahed
Department of Materials Engineering, University of Technology
Baghdad, Iraq
Email: mohanad.najm97@gmail.com

1. INTRODUCTION

Image processing can be described as performing specific mathematical processes using signal processing, with input being a picture, an image, video, image collection, or photo frame, and output being an image or a collection of the image-related parameters or characteristics [1]. Many methods of image processing include seeing images as 2-D signals and applying typical signal processing techniques. The approaches of image encryption could be classified to 2 groups depending upon the operations of spatial and frequency domains [2]. The former works in spatial domain, with encrypted artefacts such as pixel position and intensity, whereas the latter works in frequency domain using the coefficients of frequency. The prior encryption approaches work in the spatial domain. Approaches for spatial domain image encryption necessitate a large number of the calculations [3]. Digital data is represented with regard to frequencies in the transform domain. Various methods of digital watermarking in the transform domain have been published in literature. Every approach in the transform domain has its own set of benefits and drawbacks. Discrete wavelet transformation (DWT), discrete cosine transform (DCT), fast fourier transform (FFT), and discrete fourier transform (DFT) are examples of different transforms utilized in the transform domain. The watermark modifies coefficients of transform domain for inserting the watermark. Spread spectrum is considered as the 3rd watermarking approach employed. Spread spectrum is a technique for spreading the energy of the watermark across visually relevant frequency bands so that the amount of the energy in any one band is unnoticeable and small [4].

This work presents a DWT-singular value de-composition (DWT-SVD) based image encryption approach depending on approaches of digital watermarking; results showed that the presented approach can withstand almost all attacks; yet, the efficiency of the proposed scheme is unacceptably low when it comes to Gaussian noise attacks. As a result, the research will focus on applying image denoising to improve anti-attack capability against noise attacks with the use of S-transform. In the case when the signal of interest has been damaged via noise, signal denoising is necessary to retrieve information that is carried by signal with minimal error. De-noising approaches, like medial filtering [5], mean filter [6], variable digital filtering [7], and Wiener filtering [8] have been indicated. Wavelet transform has lately gained popularity as a signal de-noising approach [9], [10]. Adaptive wavelet shrinkage [11], wavelet correlation method [12], and dual-tree complex wavelet coefficient are a few of the techniques presented [13].

2. DISCRETE WAVELET TRANSFORM

Regarding the operation of image processing, wavelets were used for watermarking, compression, coding, sample edge detection, and de-noising of interesting characteristics in order to classify them afterwards. Image denoising using thresholding DWT coefficients is discussed in the following sub-sections [14]–[16]. DWT process and IDWT are discussed brifly in this section before the de-noising image process begain against AWGN attacked.

2.1. Image data discrete wavelet transformation

Images are presented as two-dimensional array of the coefficients. The degree of the brightness regarding each one of the points is represented by each coefficient. Almost all herbal images display smooth coloring variations with excellent details that depict sharp edges from the simple versions. The clean color changes could be referred to as versions of low-frequency, while pointy variations could be referred to as versions of excessive-frequency. Furthermore, components of low-frequency (for example, smooth versions) reveal image' base, whereas the components of excessive-frequency (such as, edges supplying details) were uploaded onto components of low-frequency to refine an image, resulting in in-depth images. In addition, in compared to the details, the easy versions have been considerable. Differentiating between simple variations and photograph information can be done in a variety of ways. Image decomposition using DWT re-modeling is an example of such a method. Figure 1 depicts different levels of decomposition in relation to DWT, Figure 1(a) single-level, Figure 1(b) two-level and Figure 1(c) three-level decomposition.

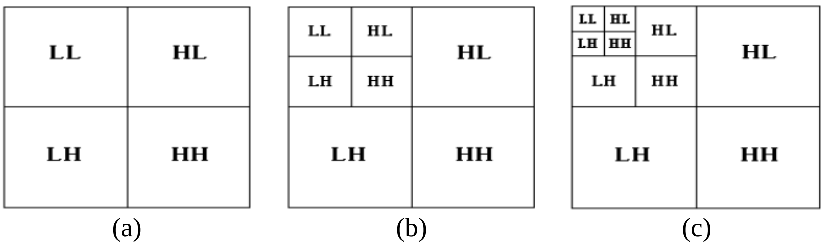

Figure 1. Levels of DWT de-composition (a) single level decomposition, (b) two level decomposition, and (c) three level decomposition [14]

2.2. Image's inverse discrete wavelet transformation

The reverse wavelet transform was used to re-create an image from a variety of data classes. During the process of re-construction, a pair of low-and high-pass filters were deployed as well. Synthesis filter pair is the name given to the filters. The process of filtering is considered as the opposite of transformation; it begins at the highest level. Filters were applied column-by-column first, then row-by-row until the lowest level was reached.

3. SINGULAR VALUE DECOMPOSITION

The SVD method is a matrix transformation method that is based on eigenvalue. Every image could be represented as matrix, which SVD might decompose to a summation of multiple matrices. While SVD isn't associated with frequency-to-spatial domain transformations, the singular image value has a high level of the stability; it is frequently combined with transformation techniques in image processing area. In a case where the disturbances have been introduced to some image, the singular value is not significantly changed. In addition, the singular vector of a matrix is invariant with regard to translation, rotation, and other operations. As a result, singular value may be effectively reflecting matrix attributes. In a case of being applied to an image's matrix, singular value, as well as its spanned vector space, may be reflecting numerous image features and components. The algebraic features of an image may be described, and SVD was widely used in image processing. Almost all current image encryption techniques are based on SVD, which has increased robustness because of its stability and rotation invariance [17], [18].

A good method to compute eigenvalues and eigenvectors of data matrix X(K×M) was by using SVD indicated in (1) [19]:

$$X = \begin{bmatrix} x_1 & x_2 \ldots\ldots\ldots\ldots & x_M \\ x_{M+1} & x_{M+2} \ldots\ldots\ldots & x_{2M} \\ x_{(K-1)M+1} & x_{(K-1)M+2\ldots\ldots} & x_{KM} \end{bmatrix} \tag{1}$$

SVD theorem states that M×M matrix X can be de-composed into products of the following matrices:

$$X = U\sum V^{*^T} \tag{2}$$

where U is a K×K ortho-normal matrix containing left singular vectors which have been ordered column by column:

$$U = \begin{bmatrix} 1 & 1 \ldots\ldots & 1 \\ u_1 & u_2 \ldots\ldots & u_K \\ 1 & 1 \ldots\ldots & 1 \end{bmatrix} \tag{3}$$

V represent M×M orthonormal matrix associated with right singular vectors:

$$V = \begin{bmatrix} 1 & 1 \ldots\ldots & 1 \\ v_1 & v_2 \ldots\ldots & v_K \\ 1 & 1 \ldots\ldots & 1 \end{bmatrix} \tag{4}$$

whereas Σ represent K×M matrix with regard to non-negative real singular values:

$$\sum \begin{bmatrix} \sigma_1 \quad 0 \ldots\ldots\ldots 0 \\ 0 \quad \sigma_2 \ldots\ldots\ldots 0 \\ \ldots\ldots\ldots\ldots\ldots\ldots. \\ \ldots\ldots\ldots\ldots\ldots\ldots. \\ 0 \quad 0 \ldots\ldots\ldots \sigma_M \\ 0 \quad 0\ldots\ldots\ldots..0 \\ \ldots\ldots\ldots\ldots\ldots\ldots. \\ \ldots\ldots\ldots\ldots\ldots\ldots. \\ 0 \quad 0\ldots\ldots\ldots..0 \end{bmatrix} \tag{5}$$

Because of the features of SVD, certain watermarking computations have been proposed for this system in the last two years. The main idea behind this method is finding SVD of the cover image and after that alter its solitary properties to add a watermark. Because some of the SVD-based computations were designated as SVD-situated, it's possible that lone SVD region was used for watermarking the image. Lately, some half-and-half SVD-based computations have been suggested, where DWT, DCT, fast hadamard transform, and other sorts of the changes space were employed so as to insert the watermark to an image [20].

4. S-TRANSFORM

S-transform represents a variant of short-time fourier transform (STFT), with frequency-dependent Gauss window replacing window function. The width of a Gauss window is inversely proportionate to frequency, whereas the height has been linearly scaled. S-transform has excellent time resolution for the components of high-frequency and sufficient frequency resolution for the components of low-frequency due to its window scaling behavior. The S-transform can be written as (6) [21]:

$$X(t,f) = \int_{-\infty}^{\infty} x(\tau).\, g(\tau - t, f).\, e^{-j2\pi f\tau} d\tau \quad (6)$$

where $x(t)$ represent the signal and $g(t,f)$ represent the frequency-dependent Gauss window, provided by [21]:

$$g(t,f) = \frac{|f|}{\sqrt{2\pi}} e^{\left(\frac{-t^2 f^2}{2}\right)} \quad (7)$$

The existence of variable f renders window spread frequency dependent. Taking under consideration the fact that $X(t,f)$is complex valued, the modulus $|X(t,f)|$ is typically plotted in practice for constructing a representation of time–frequency. The local spectrum is represented by the S-transform; consequently, averaging local spectrum throughout time yields fourier spectrum that is written as (8):

$$\int_{-\infty}^{\infty} X(t,f) dt = X(f) \quad (8)$$

The signal in the representation of time $x(t)$ is recoverable exactly from $X(t,f)$ depending on the next in [21], [22]:

$$x(t) = \int_{-\infty}^{\infty} \{\int_{-\infty}^{\infty} X(t,f) dt\} e^{j2\pi f t} df \quad (9)$$

Denoising is done in representation of time–frequency in this work, and the signal has been retrieved from noise with (9). The discrete S-transform utilized in the present work to allow for the processing in continuous S-transformation. Assuming that $x(n), n = 0, 1, \dots (N-1)$ indicate discrete time series which correspond to $x(t)$ with an interval of time sampling of T_s. S-transformation that is related to discrete time series $x(n)$ has been provided as (10):

$$X(n,k) = \sum_{m=0}^{N-1} x(m-n) e^{\frac{-2\pi^2 m^2}{k^2}} e^{\frac{-j2\pi mk}{N}} \quad (10)$$

The inverse discrete S-transformation is [23]:

$$x(n) = \frac{1}{N} \sum_{k=0}^{N-1} \{\sum_{n=0}^{N-1} X(n,k)\} e^{\frac{j2\pi nk}{N}} \quad (11)$$

5. STRATEGIES OF IMAGE DENOISING UTILIZING S-TRANSFORM

When it comes to the digital image processing, images are often under attacks by various noise types, resulting in a reduction in image quality. Whether image noise is efficiently filter out or not, it will impact consequent processing like the edge detection, image decryption, feature extraction, and object segmentation. As illustrated in Figure 2, this work proposes a denoising approach depending upon analysis of time–frequency employing S-transformation.

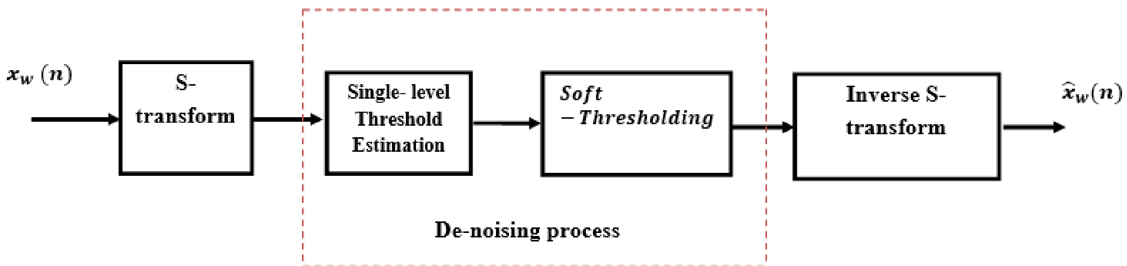

Figure 2. Flow graph of denoising process

The process of image denoising is described in the following phases: in (10) is used to apply a discrete S-transform to a noisy image (image corrupted by additive white Gaussian noise (AWGN)). S-transformation in (10) could be taken under consideration as convolution operation in frequency domain between signal X(k) and localizing scaled Gauss window (k), based on the principles of the DFT and convolution theorem. S-transformation may be written as (12):

$$X(n,k) = \sum_{m=0}^{N-1} x(m-n) e^{\frac{-2\pi^2 m^2}{k^2}} e^{\frac{-j2\pi mk}{N}} = \sum_{m=0}^{N-1} x(m-n) w(m)\, e^{\frac{-j2\pi mk}{N}}$$
$$= X(k) \underset{(k)}{*} W(k) e^{-j\frac{2\pi nk}{N}} \tag{12}$$

In the case where the image is regarded in the terms of the imaginary and real components, in (12) may be represented as (13):

$$X(n,k) = \sum_{m=0}^{N-1} x(m-n) e^{\frac{-2\pi^2 m^2}{k^2}} e^{\frac{-j2\pi mk}{N}} = \sum_{m=0}^{N-1} x(m-n) w(m)\, e^{\frac{-j2\pi mk}{N}}$$

$$= X(k) \underset{(k)}{*} W(k) e^{-j\frac{2\pi nk}{N}} \tag{13}$$

The exponential complex represented by ($e^{-j\frac{2\pi nk}{N}}$) indicates the window shift in time-domain. According to (13), frequency domain denoising process requires thresholding in the imaginary as well as the real regions of spectrum. The value of the threshold is calculated as (14):

$$\gamma_{k,re} = \xi . \sigma_{v,k,re} \sqrt{2log\ (N)}$$
$$\gamma_{k,im} = \xi . \sigma_{v,k,im} \sqrt{2log\ (N)} \tag{14}$$

In which $\sigma_{v,k,re}$ and $\sigma_{v,k,im}$ respectively represent noise standard deviation for real and imaginary parts. The kth noise standard deviation values can be estimated based on:

$$\sigma_{v,k,re} = \frac{median(|X_{re}(n,k)\ |)}{0.6745}$$
$$\sigma_{v,k,im} = \frac{median(|X_{im}(n,k)|)}{0.6745} \tag{15}$$

Following specifying threshold values for imaginary and real parts $\gamma_{k,im}$ and $\gamma_{k,re}$ the time-frequency representations of imaginary and real parts after hard thresholding include:

$$X_{\gamma,re}(n,k) = \begin{cases} X_{re}(n,k) & if|X_{re}(n,k)\ | > \gamma_{k,re} \\ 0 & if|X_{re}(n,k)| \le \gamma_{k,re} \end{cases}$$
$$X_{\gamma,im}(n,k) = \begin{cases} X_{im}(n,k) & if|X_{im}(n,k)\ | > \gamma_{k,im} \\ 0 & if|X_{im}(n,k)\ \ | \le \gamma_{k,im} \end{cases} \tag{16}$$

After soft thresholding, the time-frequency representations of imaginary and real parts can be represented as (17):

$$X_{\gamma,re}(n,k) = \begin{cases} sgn(X_{re}(n,k))\big(|X_{re}(n,k)| - \gamma_{k,re}\big) & if|X_{re}(n,k)| > \gamma_{k,re} \\ 0 & if|X_{re}(n,k)| \le \gamma_{k,re} \end{cases}$$
$$X_{\gamma,im}(n,k) = \begin{cases} sgn(X_{im}(n,k))(|X_{im}(n,k)\ | - \gamma_{k,im}) & if|X_{im}(n,k)| > \gamma_{k,im} \\ 0 & if|X_{im}(n,k)| \le \gamma_{k,im} \end{cases} \tag{17}$$

Combining imaginary and real parts yields the following time-frequency representation:

$$X_\gamma(n,k) = X_{\gamma,re}(n,k) + jX_{\gamma,im}(n,k) \tag{18}$$

The inverse discrete S-transform could be used for recovering the denoised image x(n) in time representation. Figure 3 shows the suggested denoising approach based upon S-transformation.

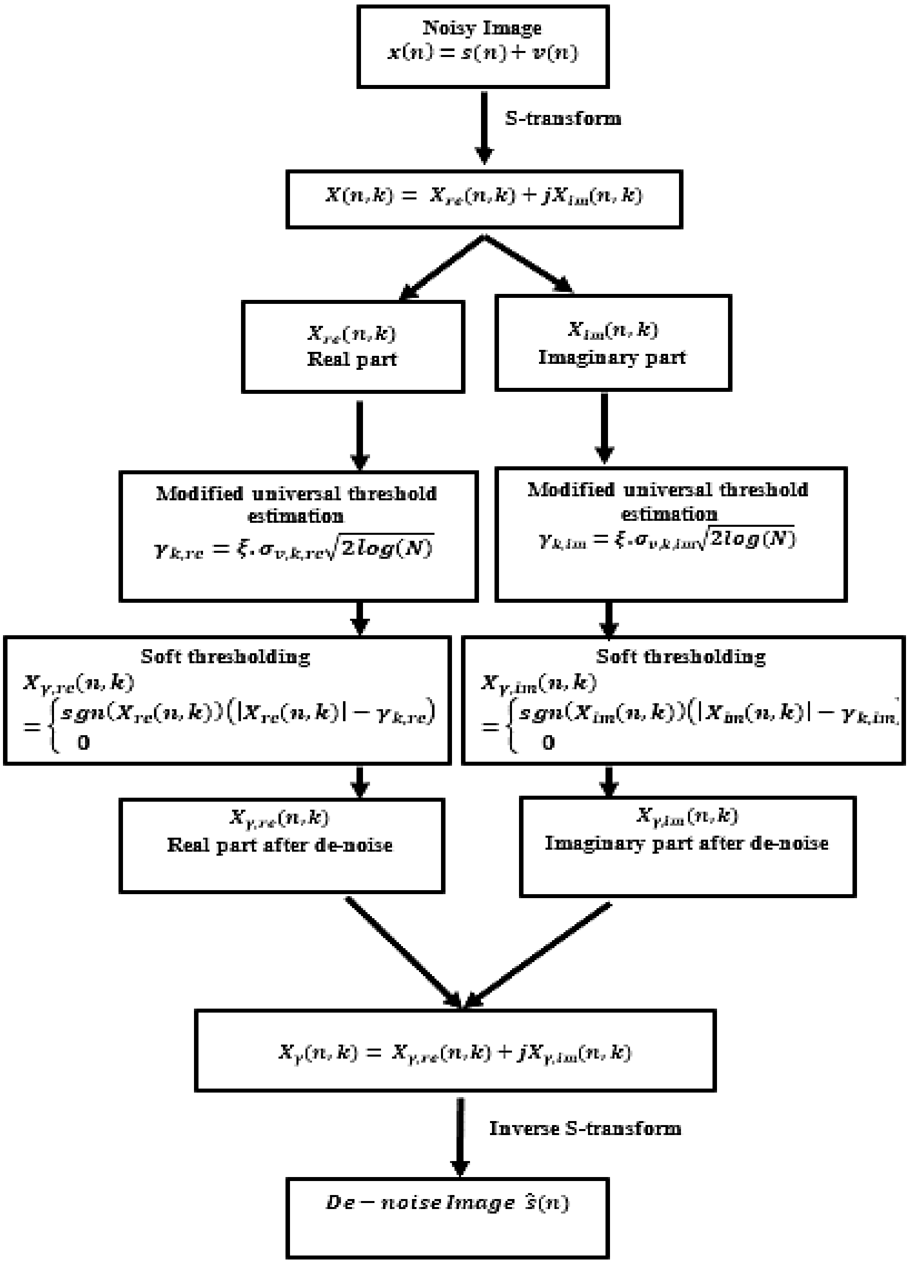

Figure 3. Image denoising diagram

6. ENCRYPTION METHODS BASED ON THE DWT-SVD THROUGH THE UTILIZATION OF THE METHODS OF DENOISING UTILIZING THE S-TRANSFORM

Utilizing de-noising methods before image decryption for increasing anti-attack capabilities connected to this method against the noise attacks, based on the proposed DWT-SVD encryption methods with usage of a normal image as the host image. In addition, in Figure 4, a new workflow was depicted. Decryption and encryption processes could be given in the next method, according to Figure 4:

- Step 1: choosing original image and host image of the same size;
- Step 2: applying DWT to both images, as well as obtaining four sub-bands for each image, utilizing SVD to each of subbands, and composing coincident subbands toward the original image and the host image; and finally, application of the inverse-DWT to obtain encrypted-image, such a processing could be referred to as DWT-SVD encryption technique;
- Step 3: denoising techniques utilizing the S-transform for filtering attacked the encrypted image during transmission;

- Step 4: the encrypted image will be decrypted, and the decryption process will be handled in the same way as the encryption inverse operation; after that, the decrypted image will be obtained.

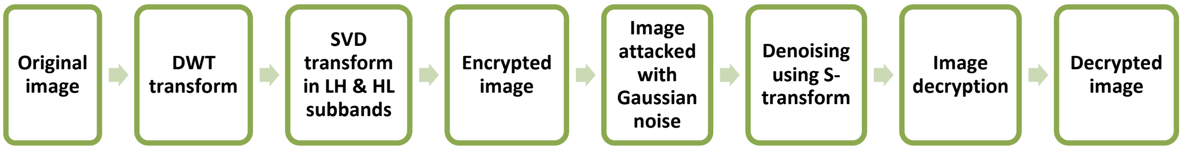

Figure 4. Suggested model

7. PERFORMANCE MEASURES

The normalized mean square error (NMSE), maximum absolute error (MAE), peak signal to noise ratio (PSNR), and mean squared error (MSE) are some of the most used image reliability measurement measures. SNR over 40 dB produces optimum image quality that is near to original image; signal to noise ratio (SNR) 30-40 dB gives great quality of an image with appropriate distortions; SNR 20-30 dB produces poor quality of an image; SNR less than 20 dB produces undesirable image [24]. In addition, the calculation approaches for the PSNR and NMSE [25] were provided as (19):

$$PSNR = 10\ log_{10} \frac{255^2}{MSE} \tag{19}$$

where MSE represent MSE between the original image (x) and de-noised one ($\hat{x}$) with an MxN size:

$$MSE = \frac{1}{M*N} \sum_{i=1}^{M} \sum_{j=1}^{N} [x(i,j) - \hat{x}(i,j)]^2 \tag{20}$$

8. RESULTS AND DISCUSSION

We used two distinct techniques to watermark digital images, and each scheme yielded three different result types, as shown in:
- Image watermarking/de-watermarking without any image attacks.
- Image watermarking/de-watermarking with Gauss noise image attack and denoising processing using S-transform.
- Image watermarking/de-watermarking with Gauss noise image attack and denoising processing using DWT.

MSE and PSNR are used to assess the quality of the recovered image. Due to slight errors in the image extraction technique, a higher PSNR value indicates a higher quality of recovered image. MSE is a similarity metric between two images that is close to zero. For illustrating the findings, we used the image buliding. Figure 5 depicts the decrypted and encrypted image. The encrypted image is definitely identical to the host image, depending on the results. In other words, the secret imag information had been efficiently hidden inside the encrypted image. The details of the secret image are plainly visible in the decrypted images. We discover that all four results fulfil our expectations, and the encryption approach depending on DWT-SVD architecture performs admirably.

On the host image, the DWT-SVD noise method was used to watermark the original image. Then, a Gauss image with variance-attacks was applied to water-mark image, after which the attack noise was removed with the use of DWT technique. After that, it was dewatered, and obtained water-marked image is shown in Figure 6.

On host image, DWT-SVD noise method was used to watermark the original image. Then, a Gauss image with variance attack was applied to water-mark image, and after that the attack noise was removed with the use of S-transform algorithm. After that, it was dewatered, and obtained water-marked image is shown in Figure 7. Table 1 compares the performance of the suggested approach employing the S-transform algorithm on noise power with a variance of 0.1 to the case without noise attack and the DWT-based denoising approach. The noise power value is used for calculating the MSE and PSNR values.

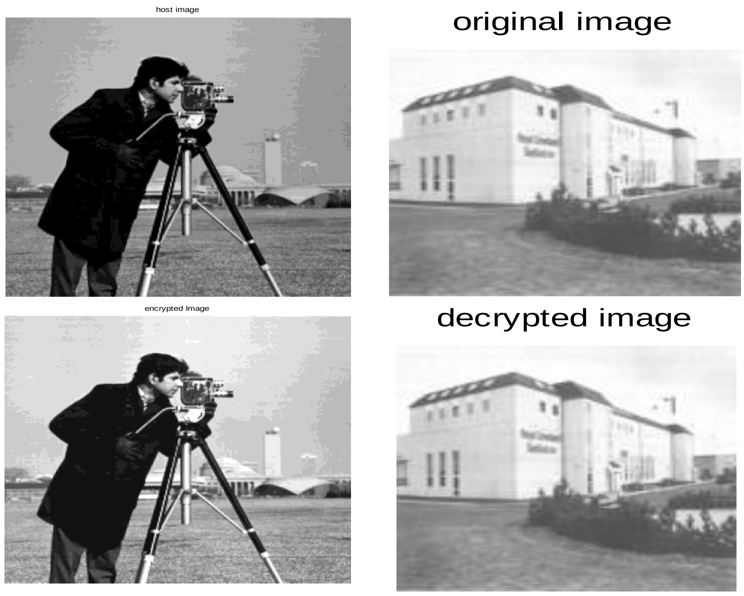

Figure 5. Results for image encryption without noise attacks

Figure 6. Results of image encryption with Gauss noise attacks and decryption utilizing the DWT process

Figure 7. Results of image encryption with Gaussian noise attacks and decryption using S-transform algorithm

Table 1. Comparison the performance of the suggested approach employing the S-transform algorithm with another method

Cases	PSNR	MSE
No. attacks	212	0
DWT based on the daubechies wavelet biases	42.30	0.008
S-transform	66.121	0.0032

9. CONCLUSION

The findings of this work reveal that DWT-SVD based watermark method, along with S-transform based de-noising algorithm, have provided the best efficiency in the presence of the recovery of the watermark image which was attacked by Gauss noise. The results were evaluated analytically in terms of PSNR and MSE, both of which were high for the new system of the DWT-SVD watermark. The MSE gives an idea of how well the de-noised signal is similar to the original signal. A suitable criterion to compare the performance of the various methods in de-noising the signals is to identify the technique that results in the highest SNR with the lowest possible MSE.

REFERENCES

[1] M. Sharkas, D. ElShafie, and N. Hamdy, “A dual digital-image watermarking technique,” in *Proceedings-WEC’05: 3rd World Enformatika Conference*, 2005, pp. 136–139.
[2] Z. Liu, “Comparative evaluations of image encryption algorithms,” Ph.D. dissertation, Dept. Comput. and Inf. Sci., Auckland Univ. of Technology, Auckland, New Zealand, 2018.
[3] Z. Liu *et al.*, “Double image encryption by using Arnold transform and discrete fractional angular transform,” *Optics and Lasers in Engineering*, vol. 50, no. 2, pp. 248–255, Feb. 2012, doi: 10.1016/j.optlaseng.2011.08.006.
[4] Y. Y. Al-Aboosi, R. S. Issa, and A. K. Jassim, “Image denosing in underwater acoustic noise using discrete wavelet transform

with different noise level estimation," *TELKOMNIKA (Telecommunication Computing Electronics and Control)*, vol. 18, no. 3, pp. 1439–1446, Jun. 2020, doi: 10.12928/telkomnika.v18i3.14381.
[5] X. Zhang and Y. Xiong, "Impulse noise removal using directional difference based noise detector and adaptive weighted mean filter," *IEEE Signal Processing Letters*, vol. 16, no. 4, pp. 295–298, Apr. 2009, doi: 10.1109/LSP.2009.2014293.
[6] R. Lukac, B. Smolka, and K. N. Plataniotis, "Sharpening vector median filters," *Signal Processing*, vol. 87, no. 9, pp. 2085–2099, 2007, doi: 10.1016/j.sigpro.2007.02.009.
[7] M. J. Alam and D. O'Shaughnessy, "Perceptual improvement of Wiener filtering employing a post-filter," *Digital Signal Processing*, vol. 21, no. 1, pp. 54–65, Jan. 2011, doi: 10.1016/j.dsp.2010.04.002.
[8] C. Wang, F. Hu, Q. He, A. Zhang, F. Liu, and F. Kong, "De-noising of wayside acoustic signal from train bearings based on variable digital filtering," *Applied Acoustics*, vol. 83, pp. 127–140, Sep. 2014, doi: 10.1016/j.apacoust.2014.04.001.
[9] K. Ghribi, M. Djendi, and D. Berkani, "A wavelet-based forward BSS algorithm for acoustic noise reduction and speech enhancement," *Applied Acoustics*, vol. 105, pp. 55–66, Apr. 2016, doi: 10.1016/j.apacoust.2015.11.011.
[10] S. Wang and X. Zeng, "Robust underwater noise targets classification using auditory inspired time–frequency analysis," *Applied Acoustics*, vol. 78, pp. 68–76, Apr. 2014, doi: 10.1016/j.apacoust.2013.11.003.
[11] Y. Xu, J. B. Weaver, D. M. Healy, and J. Lu, "Wavelet transform domain filters: a spatially selective noise filtration technique," *IEEE Transactions on Image Processing*, vol. 3, no. 6, pp. 747–758, 1994, doi: 10.1109/83.336245.
[12] S. M. Govindan, P. Duraisamy, and X. Yuan, "Adaptive wavelet shrinkage for noise robust speaker recognition," *Digital Signal Processing*, vol. 33, pp. 180–190, Oct. 2014, doi: 10.1016/j.dsp.2014.06.007.
[13] P. R. Hill, A. M. Achim, D. R. Bull, and M. E. Al-Mualla, "Dual-tree complex wavelet coefficient magnitude modelling using the bivariate Cauchy–Rayleigh distribution for image denoising," *Signal Processing*, vol. 105, pp. 464–472, Dec. 2014, doi: 10.1016/j.sigpro.2014.03.028.
[14] M. Misiti, Y. Misiti, G. Oppenheim, and J.-M. Poggi, *Wavelet toolbox*. Natick: The MathWorks Inc., 1996.
[15] D. Gupta and S. Choubey, "Discrete wavelet transform for image processing," *International Journal of Emerging Technology and Advanced Engineering*, vol. 4, no. 3, pp. 598–602, 2015.
[16] D. Baleanu, *Advances in wavelet theory and their applications in engineering, physics and technology*. Rijeka: InTech, 2012, doi: 10.5772/2668.
[17] N. M. Makbol, B. E. Khoo, and T. H. Rassem, "Block-based discrete wavelet transform-singular value decomposition image watermarking scheme using human visual system characteristics," *IET Image Processing*, vol. 10, no. 1, pp. 34–52, Jan. 2016, doi: 10.1049/iet-ipr.2014.0965.
[18] A. Mansouri, A. M. Aznaveh, and F. T. Azar, "SVD-based digital image watermarking using complex wavelet transform," *Sadhana*, vol. 34, no. 3, pp. 393–406, Jun. 2009, doi: 10.1007/s12046-009-0016-y.
[19] M. A. Cloutier, "Optimal digital detection of acoustic signals in colored noise," M.S. thesis, Dept. Sci. in Elect. Eng. and Sci. in Eng. Acoust., Naval Postgraduate School, CA, United States, 1995.
[20] D. S. Mitra and A. K. Saxena, "DCT DWT SVD image watermarking," *International Research Journal of Engineering and Technology (IRJET)*, vol. 5, no. 7, pp. 198–205, 2018.
[21] R. G. Stockwell, L. Mansinha, and R. P. Lowe, "Localization of the complex spectrum: the S transform," *IEEE Transactions on Signal Processing*, vol. 44, no. 4, pp. 998–1001, Apr. 1996, doi: 10.1109/78.492555.
[22] C. R. Pinnegar and D. W. Eaton, "Application of the S transform to prestack noise attenuation filtering," *Journal of Geophysical Research: Solid Earth*, vol. 108, no. 9, pp. 1–10, Sep. 2003, doi: 10.1029/2002JB002258.
[23] M. Schimmel and J. Gallart, "The inverse S-transform in filters with time-frequency localization," *IEEE Transactions on Signal Processing*, vol. 53, no. 11, pp. 4417–4422, Nov. 2005, doi: 10.1109/TSP.2005.857065.
[24] C. Tan, G. Seet, A. Sluzek, and D. He, "A novel application of range-gated underwater laser imaging system (ULIS) in near-target turbid medium," *Optics and Lasers in Engineering*, vol. 43, no. 9, pp. 995–1009, Sep. 2005, doi: 10.1016/j.optlaseng.2004.10.005.
[25] J. N. Ellinas, T. Mandadelis, A. Tzortzis, and L. Aslanoglou, "Image de-noising using wavelets," *TEI of Piraeus Applied Research Review*, vol. 9, no. 1, pp. 97-109, 2004.

BIOGRAPHIES OF AUTHORS

Mohanad Najm Abdulwahed is an Associate Professor at the Department of Materials Engineering, University of Technology Baghdad, Iraq, where he has been a faculty member since 2013, mohand graduated B.Eng. degree in computer science from RUC Baghdad, Iraq, an M.Sc. in Computer Science from Osmania University, Hyderabad India, as well as a lecturer at Department of Materials Engineering, University of Technology Baghdad. His research interests ar artificial intelligence, bioinformatics applications, image processing, computer vision, and information security. He can be contacted at email: mohanad.najm97@gmail.com.

Ali Kamil Ahmed was born in Baghdad, Iraq, in 1982. He received the B.Sc. degree in computer technology engineering from Electrical Engineering Technical College-Middle Technical University, and the M.Sc. degree in computer systems architecture from Isfahan University of Technology, Iran. He is currently a Lecturer in Department of Materials Engineering, University of Technology, Iraq. His current research interests include IoT, wireless networks, artificial neural networks, and image processing. He can be contacted at email: ali.k.ahmed@uotechnology.edu.iq.